Studies on the Effect of Load Variations for Three-Phase AC-DC Current Injection Hybrid Resonant Converter

Rahimi Baharom, Mohammad Nawawi Seroji, Ahmad Ihsan Mohd Yassin, Roskhatijah Radzuan, Muhamad Nabil Hidayat
Faculty of Electrical Engineering, Universiti Teknologi MARA, 40450 Shah Alam, Selangor, Malaysia
rahimi6579@gmail.com

***Abstract*—This paper presents an investigation on the effect of load variations for three-phase ac to dc current injection hybrid resonant converter. The performance of the converter was analyses with different values of output load resistor. The effect of load variations on the supply current waveforms, resonant current waveform and the output voltage waveform was observed and investigated. Apart of the waveforms, the performance of the converter was analyzed based on the total harmonics distortion (THD) level of the supply current waveform for both nominal output load operation and during increases the output load resistor. The circuit was simulated in MATLAB/Simulink environment. A 1-kW experimental test-rig was constructed to verify the output load variations studies for the three-phase ac-dc current injection hybrid resonant converter. Selected simulation and experimental results have been provided in the paper to validate the analysis.**

***Index Terms*—Three-Phase AC-DC Converter; Current Injection; Hybrid Resonant Converter.**

I. INTRODUCTION

Research in industrial electronics always focuses on the enhancement of converters efficiency and power density [1-4]. Due to the interest in high power density, encouraging the exploration of higher operating frequency. Thus, the resonant converters have been found to be a good option to the abovementioned requirement [5]. As compared to the conventional hard-switching pulse width modulation (PWM) converters, the resonant converters are capable to realize soft-switching for power switches, whilst, reducing the switching losses [6] [7].

The resonant converters can be classified into several types of configurations based on the arrangement of inductor and capacitor elements. Details circuit arrangement and characteristics of the resonant converters that have been applied in dc power supply applications have been discussed in [8]. The series resonant converter and parallel resonant converter are among two basic configurations of the resonant converters [6]. The series configuration of resonant converters has the merit of high voltage gain and high conversion efficiency. Furthermore, its switching losses decrease with load decrease. This type of circuit configuration is suitable for high output voltage with low output current applications [9]. However, the series configuration of the resonant converters suffers a wide variation range of switching frequency. As a result, the output voltage cannot be regulated at light-load or no-load condition [6] [9] [10]. In addition, the use of the series configuration of resonant converter required a larger output capacitor filter to minimize the ripple of the output voltage.

The parallel configuration of resonant converters has better output voltage regulation during light-load or no-load condition. This type of resonant converter circuit configuration is naturally short circuit proof due to the resonant tank inductor or capacitor elements [9]. It is suitable for high output current with low output voltage applications. However, the parallel configuration of resonant converters has poor efficiency at light load condition [6]. This is due to the high circulating resonant tank current resulting in higher switching losses [9]. Hence, both series and parallel circuit configurations of resonant converters incapable to utilize certain parasitic components in some applications [6].

To overcome the disadvantages of both series and parallel resonant converters, the combination series and parallel circuit configurations of resonant converter that is also called hybrid circuit configurations have been proposed [6] [7] [9]. This type of circuit configuration combines advantages of both series and parallel resonant circuit configurations and also eliminates their setbacks. Among the merit of hybrid circuit configurations of the resonant converter are their capability to operate over a large range of supply voltage, better performance of output voltage regulation and better reliability with light-load or heavy-load conditions [9] [11-12]. As compared to both series and parallel resonant converter, the hybrid resonant converter also exhibits better performance of high efficiency [11-12].

We have earlier reported, both steady-state analysis and experimentally, the three-phase ac to dc current injection hybrid resonant converter [13-14]. This paper focuses on the investigation of output load variations of the three-phase ac to dc current injection hybrid resonant converter. In order to optimize the parameters to better design the hybrid resonant converter, some steady-state models have been proposed in the previous papers [13-14] will be utilized. This steady-state model described the relationship among the load, the output voltage, and the switching frequency of the proposed converter. A prototype of 1-kW is developed based on a computer simulation model that uses MATLAB/Simulink to verify the proposed investigations.

II. COMPUTER SIMULATION MODEL

A 1-kW computer simulation model of the converter is modelled using MATLAB/Simulink to verify the effectiveness of the proposed converter. Table 1 shows the

design parameters of the proposed converter.

Figure 1 shows the top level main model of the three-phase ac to dc current injection hybrid resonant converter. The parameters used in the [13-14] is used to investigate the behavior of the proposed converter.

The modelling of three-phase diode bridge rectifier arrangement in MATLAB/Simulink is shown in Figure 2. As can be seen, the three-phase diode bridge rectifier consists of three input presented by VR, VY and VB whilst the two output are presented by +VDC and -VDC respectively. Since, the current injection technique is used to improve the power factor of the proposed converter, where the $I_{res}/3$ will be used to inject back to the junctions of the three-phase diode-bridge rectifier, therefore the modelling of three-phase diode bridge rectifier also consists of another three input presented by VR1, VY1 and VB1. The two output +VDC and -VDC are connected to the positive and negative high-frequency inverter block set respectively.

Modelling of the high-frequency half-bridge inverter with autotransformer is shown in Figure 3. By referring to Figure 3, the Mosfet1 and Mosfet2 are used to drive the inverter which is connected to the DC-link capacitors Cdc1 and Cdc2 respectively. An autotransformer is then connected to the output of the high-frequency half-bridge inverter. The modelling of single-phase high-frequency diode bridge rectifier with a DC capacitor using MATLAB/Simulink is as shown in Figure 4. The two inputs of diode bridge rectifier are presented by +Vin and -Vin respectively whilst +Vo and -Vo presented the two outputs of the diode bridge rectifier. A dc capacitor, Co is connected across the +Vo and -Vo.

Figure 5 shows the load resistor arrangement for the load step change of the proposed converter. Two resistors presented by RL1 and RL2 are connected in parallel, that is used to represented light-load and heavy-load respectively. An ideal switch which is controlled by a Step block set is then connected in series with the RL2.

Table 1
Design Parameters

Quantity	Values
Supply voltage, V_s	40 V_{rms}
Nominal output voltage, V_o	47 V
Nominal output power, P_o	1000 W
Switching frequency, f_s	20 kHz
Load resistor, R_{L1}	2.2 Ω
Load resistor, R_{L2}	100 Ω

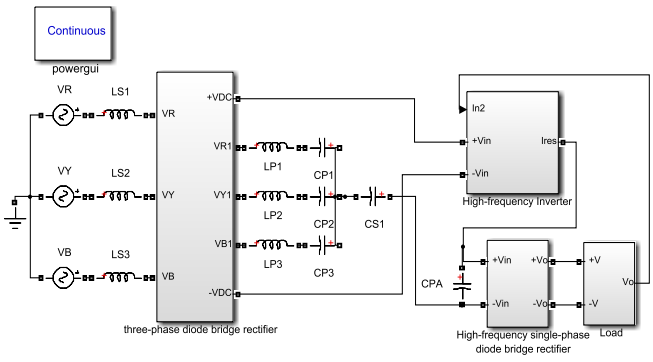

Figure 1: The top level main model of the three-phase ac to dc current injection hybrid resonant converter

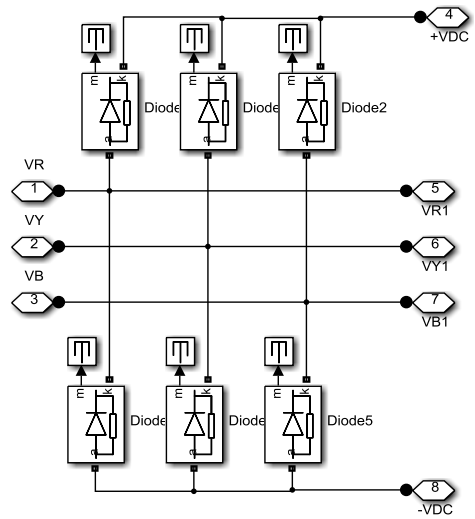

Figure 2: The three-phase diode bridge rectifier arrangement

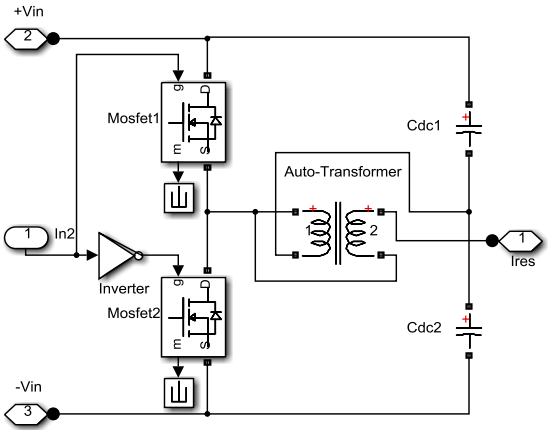

Figure 3: The high-frequency half-bridge inverter with autotransformer

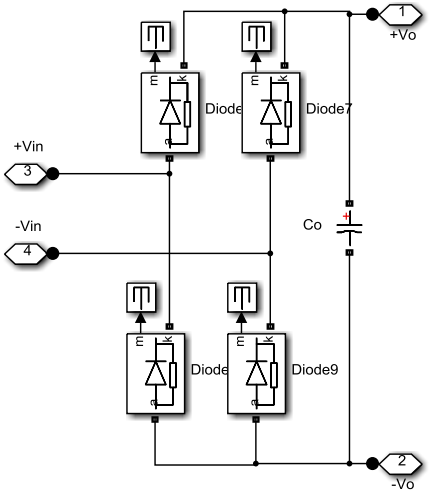

Figure 4: The single-phase high-frequency diode bridge rectifier with a DC capacitor

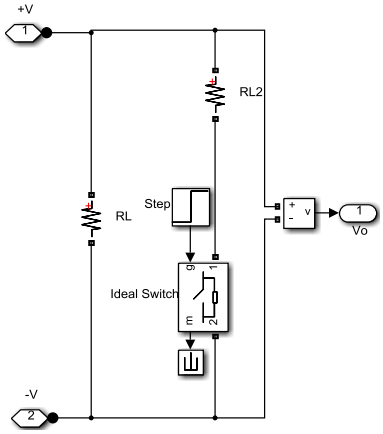

Figure 5: The load resistor arrangement

III. EXPERIMENTAL TEST-RIG

The construction of a 1-kW experimental test-rig as shown in Figure 6 used to verify the proposed converter. The hardware design was outlined completely with the power circuits, gate drives and its pulse width modulation (PWM) control circuits. The construction and component design of the experimental test-rig for three-phase AC-DC CIHRC were organized as; a) three-phase diode bridge, b) power switches, c) DC link capacitor, d) resonant tank, e) output full-bridge rectifier and f) line inductor.

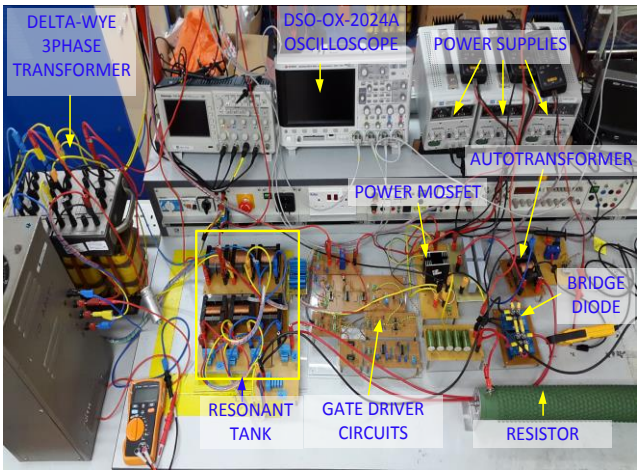

Figure 6: The experimental test-rig set-up

IV. RESULTS AND DISCUSSION

The results of the investigation of output load variations of three-phase ac to dc CIHRC are present according to nominal output load operation and by increasing the value of output load resistor. Figure 7 shows the supply current waveforms of three-phase ac to dc CIHRC during nominal output load operation. It is clearly shown that the supply current waveform is continuous, sinusoidal and in-phase with the supply voltage waveforms.

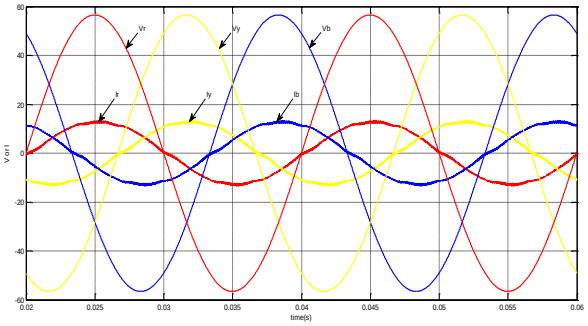

Figure 7: The simulation results of three-phase supply voltages and currents waveforms for nominal output load condition

The efficiency, power factor and the THD level of the converter have been calculated based on Equation (1) to (7).

$$\eta = \frac{P_{OUT}}{P_{IN}} \tag{1}$$

Where the output power, P_{OUT} can be determined using equation as below;

$$P_{OUT} = \frac{V_{OUT}{}^2}{R_L} \tag{2}$$

The input power, P_{IN} can be calculated as;

$$P_{IN} = 3 \times V_{RMS} \times I_{LINE_{RMS}} \times \cos\phi \tag{3}$$

Where ϕ is the displacement power factor, D.F and can be calculated using equation below,

$$D.F = \frac{powerfactor, p.f}{\gamma} \tag{4}$$

The power factor, p.f can be calculated based on the equation as below,

$$p.f = \frac{P_{IN}}{S_{IN}} \tag{5}$$

Where S_{IN} can be calculated as;

$$S_{IN} = 3 \times V_{P_{RMS}} \times I_{RMS} \tag{6}$$

Where γ can be calculated from the total harmonic distortion as follows;

$$\gamma = \sqrt{\frac{1}{THD^2 + 1}} \tag{7}$$

Noted that the normal operation of the converter is designed with the load resistor of 2.2Ω. The total harmonic distortion (THD) level for the nominal output load operation is 1.47% with the efficiency of 92.4%. Such value of THD level is well below the acceptable limit that was defined by IEEE 519 Standard.

Figure 8 shows the simulation result of the converter resonant current and voltage waveforms. Based on Figure-8, the resonant current lag the resonant voltage, thus verified that the converter operated under virtually lossless zero voltage switching (ZVS) condition. The output voltage of the three-phase ac to dc CIHRC is as shown in Figure 9. The simulation results obtained from MATLAB/Simulink are verified by experimental results as shown in Figures 10 to 12. It was observed that there was good agreement between the characteristics of the simulation and experimental results. The error of the comparison results especially for the experimental test rig was within a few percent attributed to the losses that were not included in the analysis and the component tolerance.

The results of increase output load resistor are shown in Figures 13 to 15. In this work, the value of output load resistor was increased up to 100Ω, to investigate the effect of the supply current waveforms, the resonant current and voltage waveforms and the behavior of the output voltage waveform. Figure 13 shows the simulation result of the three-phase supply currents and supply voltages waveforms for the output load resistor increases from 2.2Ω to 100Ω. Compared to the result obtained during nominal output load operation, the amplitude of the supply currents waveforms reduced from 12A to 6.7A.

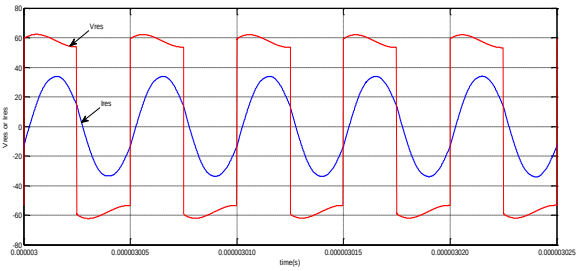

Figure 8: The simulation result of V_{res} and I_{res} for nominal output load condition

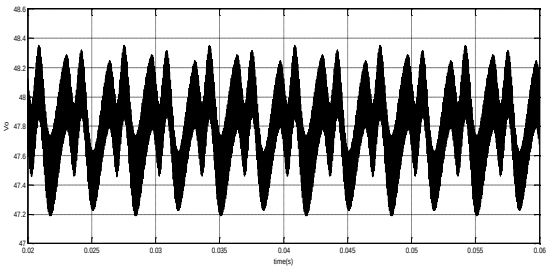

Figure 9: The simulation result of V_o for nominal output load condition

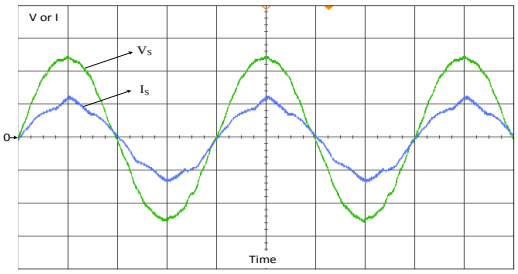

Figure 10: The experimental results of the red phase supply voltage (25 V/div, 5 ms/div) and current waveform (10 A/div, 5 ms/div) for nominal output load condition

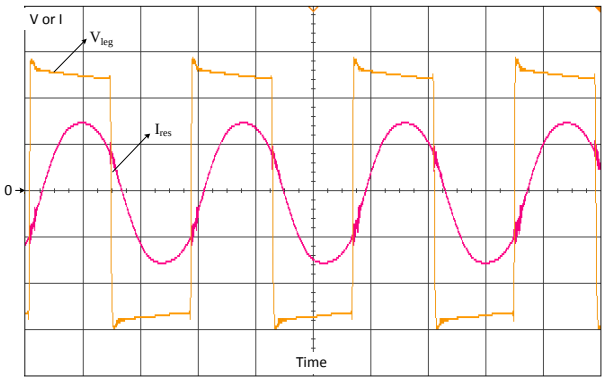

Figure 11: The experimental results of the converter resonant current (20 A/div, 16 µs/div) and switching leg voltage (22 V/div, 16 µs/div) for nominal output load condition

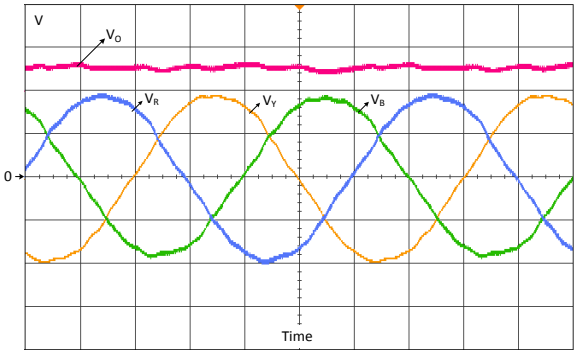

Figure 12: The experimental results of the Converter output voltage (18 V/div, 3.3 ms/div) and supply voltages (30 V/div, 3.3 ms/div) waveforms for nominal output load condition

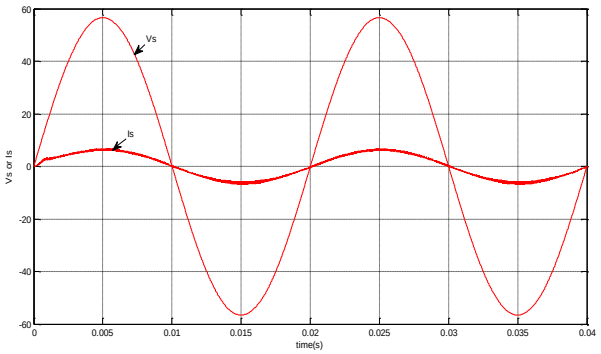

Figure 13: The simulation result of the three-phase supply currents and supply voltages waveforms for the output load resistor increases from 2.2Ω to 100Ω

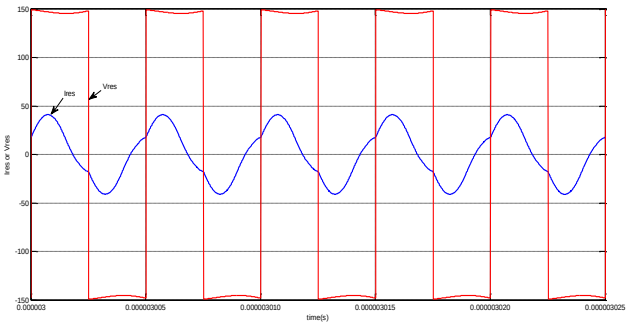

Figure 14: The simulation result of the resonant current and voltage waveforms for the output load resistor increases from 2.2Ω to 100Ω

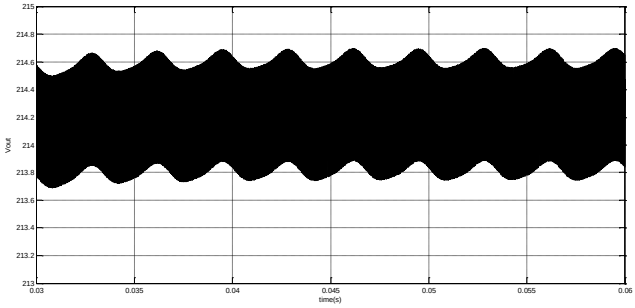

Figure 15: The simulation result of the output voltage waveform for the output load resistor increases from 2.2Ω to 100Ω

Figure 14 shows the simulation result of the resonant current and voltage waveforms for the output load resistor increases from 2.2Ω to 100Ω. It is clearly shown that the resonant current, I_{res} leads the resonant voltage, V_{res}. In addition, the amplitude of the resonant voltage increases up to 150V compared to about 60V during the nominal load resistor operation. The simulation of the output voltage waveform for the output load resistor increases from 2.2Ω to 100Ω is as shown in Figure 15. It shows that the output voltage increases up to 214V as compared to 47V during the nominal load resistor operation. Table 2 summarized the results obtained during the nominal load resistor operation and for the output load resistor increases from 2.2Ω to 100Ω.

At nominal output load operation, the converter performs as zero voltage switching (ZVS) since the resonant current, I_{res} lags the switching leg voltage, V_{leg} as illustrated in Figures 8 and 11. This is different during the output load resistor increases from 2.2Ω to 100Ω, where the resonant current, I_{res} leads the switching leg voltage, V_{leg}, as shown in Figure 14, resulting in the converter, operates under zero current switching (ZCS) condition. The total harmonic distortion (THD) level for the nominal output load operation is 1.47% with the efficiency of 92.4%. Such value of THD level is well below the acceptable limit that was defined by IEEE 519 Standard. This value increases up to 4.4% when the output load resistor increases from 2.2Ω to 100Ω, thus the efficiency of the converter decreases to 61%.

Table 2
Results of Output Load Resistor Variations

Parameters	Nominal load operation	Increase load resistor
Load Resistor, R_L	2.2Ω	100Ω
THD (%)	1.47	4.4
Efficiency (%)	92.4	61
Output voltage (V)	47	214

V. CONCLUSION

This paper has investigated the output load variations of the three-phase ac to dc current injection hybrid resonant converter. There are two parameters of the load resistor, R_L to investigate the load conditions of the proposed converter. First is during the nominal output load operation and the second is during the output load resistor increases from 2.2Ω to 100Ω condition. Since the normal operation of the converter is designed for the load resistor of 2.2Ω, thus the nominal output load operation that uses the load resistor of 2.2Ω results with low THD level (1.47%) of the supply current waveform with high power converter efficiency (92.4%). However, for output load resistor increases from 2.2Ω to 100Ω condition the THD level of the supply current waveform increases to 4.4%, with the power converter efficiency also decreases to 61%.

ACKNOWLEDGMENT

Authors gratefully acknowledge the financial support from Ministry of Higher Education Malaysia and Institute of Research Management and Innovation (IRMI) Universiti Teknologi MARA Grant No: 600-RMI/FRGS 5/3 (70/2015).

REFERENCES

[1] Ramanujam Ramabhadran, Xu She, Yehuda Levy, John S. Glaser, Ravisekhar Raju, Rajib Datta, "Universal AC Input High-Density Power Adapter Design With a Clamped Series-Resonant Converter," *IEEE Transactions on Industry Applications*, 2016, pp. 4096 – 4107.

[2] Xiaofeng Lyu, Na Ren, Yanchao Li, Dong Cao, "A SiC-Based High Power Density Single-Phase Inverter With In-Series and In-Parallel Power Decoupling Method," *IEEE Journal of Emerging and Selected Topics in Power Electronics*, 2016, pp. 893–901.

[3] Sergio Carlo, Saibal Mukhopadhyay, "A High Power Density Dynamic Voltage Scaling Enabling a Single-Inductor Four-Output Regulator Using a Power-Weighted CCM Controller and a Floating Capacitor-Based Output Filter," *IEEE Transactions on Power Electronics*, 2016, pp. 4252–4264.

[4] Zhongming Ye, John C. W. Lam, Praveen K. Jain, Paresh C. Sen, "A Robust One-Cycle Controlled Full-Bridge Series-Parallel Resonant Inverter for a High-Frequency AC (HFAC) Distribution System," *IEEE Transactions on Power Electronics*, 2007, pp.2331-2343.

[5] Xing Tan, Xinbo Ruan, "Equivalence Relations of Resonant Tanks: A New Perspective for Selection and Design of Resonant Converters," *IEEE Transactions on Industrial Electronics*, 2016, pp. 2111–2123.

[6] Mohamed Z. Youssef, Praveen K. Jain, "A Novel Single Stage AC–DC Self-Oscillating Series-Parallel Resonant Converter," *IEEE Transactions on Power Electronics*, 2006, pp. 1735–1744.

[7] Baharom, R., Omar, M.F., Wahab, N., Salleh, M. and Seroji, M.N., "A Study on the Effect of Load Variation on Quality Factor for Single Phase Half-Bridge Resonant Converter," *International Journal of Simulation: Systems, Science and Technology*, 2013, pp. 53-60.

[8] Ahmed A. Aboushady, Khaled H. Ahmed, Stephen J. Finney, Barry W. Williams, "Linearized Large Signal Modeling, Analysis, and Control Design of Phase Controlled Series-Parallel Resonant Converters Using State Feedback," *IEEE Transactions on Power Electronics*, 2013, pp. 3896–3911.

[9] Bor-Ren Lin, Shih-Kai Chung, "New Parallel ZVS Converter With Less Active Switches and Smaller Output Inductance," *IEEE Transactions on Power Electronics*, 2014, pp. 3297–3307.

[10] Rui Yang, HongFa Ding, Yun Xu, Lei Yao, Ying Meng Xiang, "An Analytical Steady-State Model of LCC type Series–Parallel Resonant Converter With Capacitive Output Filter," *IEEE Transactions on Power Electronics*, 2014, pp. 328–338.

[11] R. L. Steigerwald, "A comparison of half-bridge resonant converter topologies," *IEEE Transactions on Power Electronics*, 1988, pp. 174–182.

[12] Rahimi Baharom, Mohammad Nawawi Seroji, Mohd Khairul Mohd Salleh, "Computer simulation model and performance analysis of high power factor three-phase AC-DC current injection hybrid resonant converter," *IEEE 10th Conference on Industrial Electronics and Applications (ICIEA)*, 2015, pp. 1403 – 1407.

[13] Rahimi Baharom, Mohammad Nawawi Seroji, Mohd Khairul Mohd Salleh, Khairul Safuan Muhammad, "A high power factor three-phase AC-DC current injection hybrid resonant converter," *IECON 2016 - 42nd Annual Conference of the IEEE Industrial Electronics Society*, 2016, pp. 3123–3128.

[14] Kuntal Mandal, Soumitro Banerjee, Chandan Chakraborty, "Symmetry-Breaking Bifurcation in Series-Parallel Load Resonant DC-DC Converters," *IEEE Transactions on Circuits and Systems I: Regular Papers*, 2013, pp.778–787.